

## Complexity in the bifurcation structure of homoclinic loops to a saddle-focus

S V Gonchenko<sup>†</sup>, D V Turaev<sup>†</sup>, P Gaspard<sup>‡</sup> and G Nicolis<sup>‡</sup>

<sup>†</sup> Scientific Research Institute for Applied Mathematics and Cybernetics, Ul'janova Street 10, 603005 Nizhnii Novgorod, Russia

<sup>‡</sup> Centre for Nonlinear Phenomena and Complex Systems, Université Libre de Bruxelles, Campus Plaine, Code Postal 231, Boulevard du Triomphe, B-1050 Bruxelles, Belgium

Received 18 April 1996, in final form 4 December 1996

Recommended by R S MacKay

**Abstract.** We report on the study of bifurcations of multi-circuit homoclinic loops in two-parameter families of vector fields in the neighbourhood of a main homoclinic tangency to a saddle-focus with characteristic exponents  $(-\lambda \pm i\omega, \gamma)$  satisfying the Shil'nikov condition  $\lambda/\gamma < 1$  ( $\lambda, \omega, \gamma > 0$ ). We prove that one-parameter subfamilies of vector fields transverse to the main homoclinic tangency (1) may be tangent to subfamilies with a triple-circuit homoclinic loop; (2) may have a tangency of an arbitrarily high order to subfamilies with a multi-circuit homoclinic loop. These theorems show the high structural instability of one-parameter subfamilies of vector fields in the neighbourhood of a homoclinic tangency to a Shil'nikov-type saddle-focus. Implications for nonlinear partial differential equations modelling waves in spatially extended systems are briefly discussed.

PACS number: 0545

### 1. Introduction

The classification of vector fields according to their topological properties is a major preoccupation in the theory of dynamical systems. Many works have been devoted to the topological description of the orbits of families of vector fields such as

$$\dot{x} = X_\mu(x). \quad (1)$$

Early works have shown that hyperbolic systems are structurally stable in the sense that there exists a homeomorphism of phase space which maps the orbits of a system  $X_\mu$  onto the orbits of a perturbed system  $X_{\mu'}$  in the neighbourhood of  $X_\mu$  [1]. It was also discovered that hyperbolic systems may sustain chaotic dynamical behaviours which have become a central theme in natural sciences [2].

On the other hand, vector fields may undergo abrupt transitions between different dynamical regimes, for instance, through the Andronov–Hopf bifurcation or the tangent bifurcation which provide the simplest examples of structural instability. Generic families of vector fields undergoing such simple bifurcations were found to be locally topologically equivalent to universal families of vector fields which are completely described by a finite number of bifurcation parameters [1]. Therefore, a *complete topological description* is available, on the one hand for the hyperbolic systems and, on the other for the simple bifurcations.

However, it turns out that most dynamical systems are non-hyperbolic and display structurally unstable homoclinicities leading to intrinsically complex bifurcations between different chaotic dynamical behaviours. A systematic and comprehensive study of structurally unstable homoclinic orbits was pioneered and developed by Shil'nikov and co-workers since the mid-1960s [3–6]. Today, the methods developed by Shil'nikov and co-workers have become essential to our understanding of chaotic attractors both in discrete-time mappings [7] and in continuous-time systems such as the Lorenz and the Rössler flows [8–11]. Of considerable importance in this context is also the work of Newhouse on the existence of infinitely many sinks in nonhyperbolic systems [12–14].

The present paper is devoted to the problem of the completeness of the description of bifurcations near structurally unstable homoclinic orbits. By completeness, we mean the possibility of finding a generic family of vector fields depending only on a finite number of parameters. The impossibility of complete description of three-dimensional systems with homoclinic tangencies was proved in [14] (a similar result has been announced in [15] for the general multi-dimensional case). In the present paper, we report a study of this problem for homoclinic loops of a saddle-focus stationary point.

Consider a smooth three-dimensional dynamical system,  $X$ , satisfying the following conditions:

- (a)  $X$  possesses a stationary point  $O$  of the saddle-focus type; i.e. the characteristic exponents  $\nu_1, \nu_2, \nu_3$  of  $O$  are such that  $\nu_3 = \gamma > 0$ ,  $\nu_{1,2} = -\lambda \pm i\omega$  ( $\lambda > 0$ ,  $\omega > 0$ );
- (b) the saddle index  $\rho = \lambda/\gamma$  is less than 1.

The unstable manifold  $W^u$  of  $O$  is one-dimensional. The point  $O$  divides it into two branches called *separatrices*. All orbits of the two-dimensional stable manifold  $W^s$  have a shape of spirals tending to  $O$  as  $t \rightarrow +\infty$ . We suppose that the following condition is also satisfied.

- (c) One of the separatrices (we denote it as  $\Gamma$ ) comes back to  $O$  as  $t \rightarrow +\infty$ , forming a homoclinic loop (figure 1).

Let us consider a sufficiently small neighbourhood,  $U$ , of the loop in the form of a solid torus composed by a small neighbourhood,  $U_0$ , of the point  $O$  and a handle  $U_1$  glued to  $U_0$ . We are interested in the bifurcations of orbits lying in  $U$ . Since systems with homoclinic loops of a saddle-focus form surfaces of codimension one in the space of dynamical systems, the standard way to study bifurcations of such a system is to include it

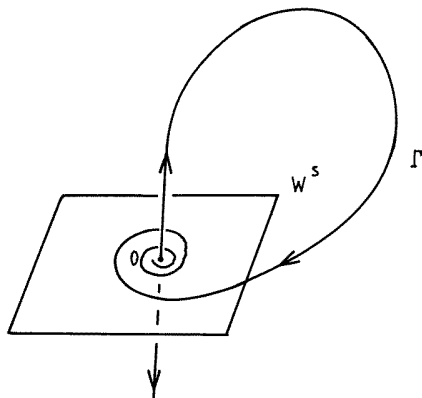


Figure 1. Schematic representation of a homoclinic loop  $\Gamma$  to a saddle-focus  $O$ .

within a one-parameter family  $X_\mu$  where  $\mu$  controls the splitting of the loop. The parameter  $\mu$  can be defined as the distance between the point of intersection of  $\Gamma$  with some surface of section and the line of intersection of  $W^s$  with the same surface of section. In this respect, the system forms a loop when  $\mu = 0$ .

When  $\mu$  varies, multi-circuit homoclinic loops can appear, which are orbits coming back to  $O$  after several passages along the handle  $U_1$ . In a one-parameter family, bifurcations of such loops have already been studied in [16–19]. In the present paper, we study bifurcations of homoclinic loops in two-parameter families, and we choose the saddle index  $\rho$  as a second control parameter.

This choice is justified by the fact that the structure of the non-wandering set of systems with homoclinic loops of a saddle-focus depends essentially upon the saddle index  $\rho$  [3, 4]. Systems with different values of  $\rho$  are not topologically equivalent, so that  $\rho$  is a genuine bifurcation parameter. Moreover, we shall show that the bifurcations of multi-circuit loops in a one-parameter family,  $X_\mu$ , depend on the value of the saddle index  $\rho$ .

We start with the bifurcations of double-circuit loops. As shown in [16], the region  $\mu > 0$ —which corresponds to the inward splitting of the loop—possesses a countable set of smooth curves  $L_j^\alpha$  ( $\alpha = 0, 1$ ) of the form  $\mu = f_j^\alpha(\rho) \sim \exp[-\frac{2\pi\rho}{\omega}(j - \frac{1-\alpha}{2})]$  which correspond to the existence of double-circuit loops  $\Gamma_j$  (where the index  $j$  means that the loop circles  $j$  times around  $O$ , see figure 2). In the cases where  $\rho$  is close to 1 and to 0 (the last case corresponding to a pair of pure imaginary characteristic exponents of  $O$ ) the behaviour of the curves  $L_j^\alpha$  was studied in [20, 21] (see also [22]). It turns out that  $L_j^1$  and  $L_j^0$  merge at some value  $\rho = \rho_j^*$  (the greater  $j$ , the closer  $\rho_j^*$  is to 1). On the other hand,  $L_j^1$  and  $L_j^0$  have different terminating points at  $\rho = 0$  (figure 3).

We see that if  $\rho$  lies between 0 and 1, the sequence of bifurcations of double-circuit loops is the same for all the values of  $\rho$  in  $]0, 1[$ . However, this property does not extend to the triple-circuit loops. We show that for sufficiently large  $j$ , in the region bounded by  $L_{j+1}^0$  and  $L_j^1$  there exist smooth curves  $L_{jk}^\alpha$ ,  $\alpha = 0, 1$ , corresponding to the existence of

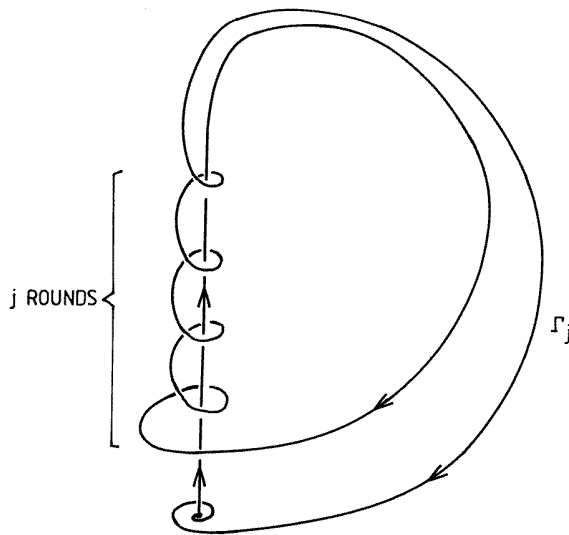


**Figure 2.** Double-circuit homoclinic loop  $\Gamma_j$  to the saddle-focus  $O$ . The integer  $j$  denotes the number of rounds during the intermediate passage around  $O$ .

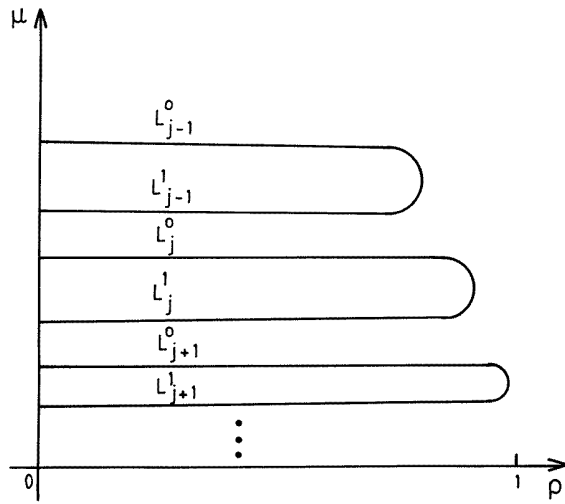


**Figure 3.** Bifurcation diagram of the double-circuit homoclinic loops  $\Gamma_j$  in the parameter plane  $(\mu, \rho)$ .  $L_j^\alpha$  with  $\alpha = 0, 1$  are the lines where the double-circuit homoclinic tangencies occur.

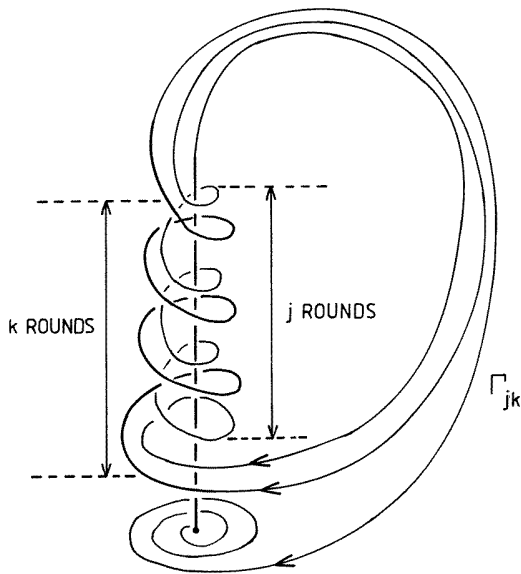


**Figure 4.** Triple-circuit homoclinic loop  $\Gamma_{jk}$  to the saddle-focus  $O$ . The integers  $j$  and  $k$  denote the numbers of rounds during the first and second intermediate passages around  $O$ .

triple-circuit loops  $\Gamma_{jk}$ ; i.e. loops which start from  $O$ , pass along the handle  $U_1$ , circle  $j$  times around  $O$ , pass along  $U_1$  again, circle  $k$  times around  $O$ , pass along  $U_1$  once more to finally reach  $O$  (figure 4). Each of these bifurcation curves lies entirely at the left-hand side of a vertical line at some value  $\rho = \rho_{jka}^*$ , where a tangency occurs (figure 5). The

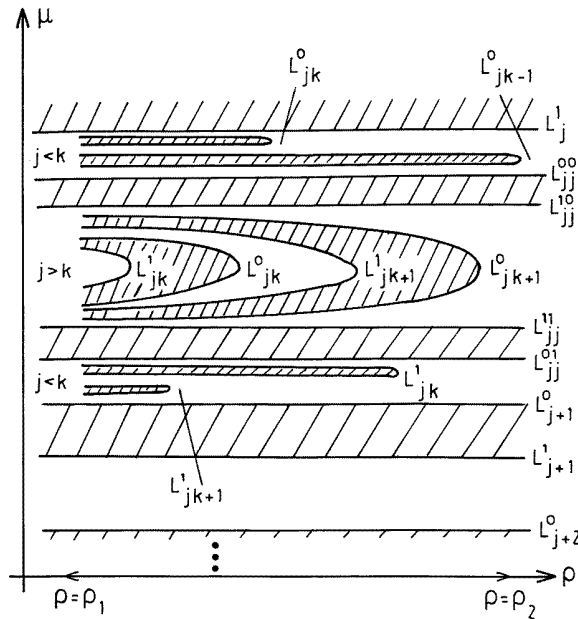


**Figure 5.** Bifurcation diagram of the triple-circuit homoclinic loops  $\Gamma_{jk}$  in the parameter plane  $(\mu, \rho)$ .  $L_{jk}^\alpha$  with  $\alpha = 0, 1$  are the lines where the triple-circuit homoclinic tangencies occur.  $\rho_{jk\alpha}^*$  are the critical parameter values where the curves  $L_{jk}^\alpha$  terminate as parameter  $\rho$  increases.

following asymptotic behaviours hold

$$\rho_{jk\alpha}^* = \frac{k}{j} + \left[ \tau(\rho_{jk\alpha}^*) - \frac{\alpha}{2} \right] \frac{1}{j} + \dots \quad \text{for } j > k \tag{2}$$

and, when  $j < k$ ,

$$\rho_{jk\alpha}^* = \frac{j}{k - \frac{1}{2}} + \left[ \tau(\rho_{jk\alpha}^*) + \frac{\alpha}{2} \right] \frac{1}{k} + \dots \quad \text{for } j < k \tag{3}$$

where  $\tau(\rho)$  is a smooth function determined by the system at  $\mu = 0$  (see equation (26) below). These implicit equations admit solutions when  $j$  and  $k$  are large enough such that  $\frac{k}{j}$ , or respectively  $\frac{j}{k}$ , remain separated from 0 and 1.

Therefore, the following picture emerges within any given small segment  $0 < \rho_1 < \rho < \rho_2 < 1$ : in any strip between  $L_{j+1}^0$  and  $L_j^1$ , there is a finite number of curves  $L_{jk}^\alpha$  consisting of two components which are either ‘parallel’ to the  $\rho$ -axis or are connected together and have a parabola-like shape.

The number of curves of both types grows linearly with the integer  $j$ . The set  $\{\rho_{jk\alpha}^*\}$  taken for  $j, k$  large enough is a dense set in the segment  $[0, 1]$ . Therefore, we have

**Theorem 1.** *Let  $X_\mu$  be a one-parameter subfamily of  $X_{\mu,\rho}$  with the curve  $\{(\mu, \rho) | \rho = \varphi(\mu)\}$  being transverse to the line  $\mu = 0$ . There exists a small variation  $\rho = \varphi(\mu) + \delta$  which makes  $X_\mu$  to be tangent to some line of existence of a triple-circuit homoclinic loop.*

When multi-circuit homoclinic loops are considered, the structure of the corresponding set of bifurcation curves becomes more complicated in the plane  $(\mu, \rho)$ . Indeed, folded lines of nine-circuit loops accumulate at the lines of triple-circuit loops in a way similar

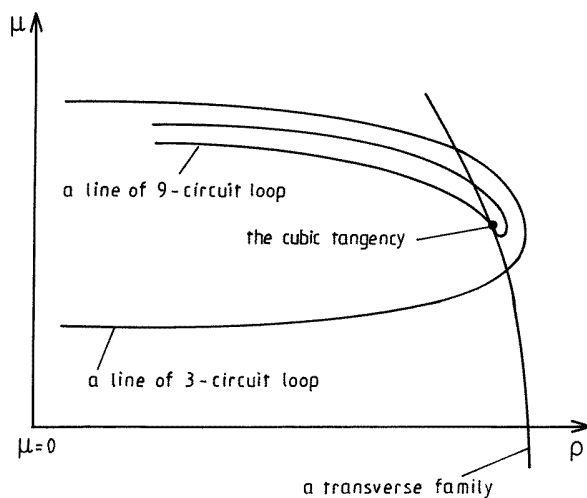


**Figure 6.** Formation of a cubic tangency between a one-parameter family of vector fields transverse to  $\mu = 0$  and a line of nine-circuit homoclinic tangency.

to the accumulation of the folded (parabola-like) lines of triple-circuit at the line of single-circuit loops ( $\mu = 0$ ). It is geometrically evident (see figure 6) that any curve transverse to  $\mu = 0$  can be varied (in a more general way than in theorem 1) in order to achieve a cubic tangency with some of these lines of nine-circuit loops.

Actually, the following general statement holds:

**Theorem 2.** Consider a one-parameter subfamily of vector fields,  $X_{\mu,\rho}$  with  $\rho = \varphi(\mu)$ , which is transverse to the line  $\mu = 0$  in the plane  $(\rho, \mu)$ . Then, a small smooth perturbation of the curve  $\rho = \varphi(\mu)$  may have a tangency of an arbitrarily high order with some of the lines of existence of homoclinic loops.

This theorem shows the arbitrarily high structural instability of one-parameter families of vector fields near homoclinic loops of a saddle-focus. As discussed below, this result turns out to have interesting consequences for nonlinear partial differential equations modelling travelling waves in spatially extended systems.

The paper is arranged as follows. In section 2, the homoclinic flow is reduced to a Poincaré map. The double circuit loops are analysed in section 3. Section 4 contains the study of the triple-circuit loops and the proof of theorem 1. We proceed to the study of multi-circuit loops and to the proof of theorem 2 in section 5. We conclude with some remarks in section 6.

## 2. The construction of the Poincaré map

Now, we proceed to the proof of the results presented above. The first step is to reduce the problem to the study of the Poincaré map. To construct this map we first note that, near the saddle-focus, the system  $X_{\mu,\rho}$  can be written in the following form [23, 24]:

$$\begin{aligned} \dot{x} &= -\lambda x - \omega y + O[(x^2 + y^2)z] \\ \dot{y} &= +\omega x - \lambda y + O[(x^2 + y^2)z] \\ \dot{z} &= \gamma z. \end{aligned} \tag{4}$$

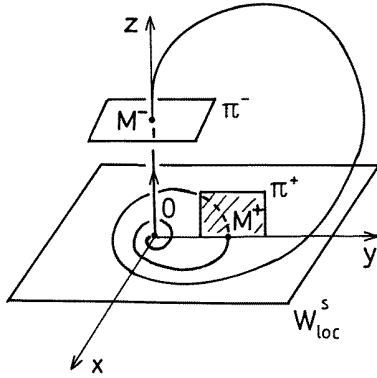


**Figure 7.** Geometric construction in the phase space  $(x, y, z)$  of the Poincaré map  $T : \Pi^+ \rightarrow \Pi^- \rightarrow \Pi^+$  generated by the flow near the homoclinic loop  $\Gamma$ .

In these coordinates, the stable manifold coincides locally with the plane  $z = 0$  and the unstable manifold with the axis  $x = y = 0$ . We chose these coordinates because it is known [23, 24] that the solutions of the system behave near  $O$  as if the system was locally linear. Thus, the solution starting from the point  $(x_0, y_0, z_0)$  at  $t = 0$  can be written in the form

$$\begin{aligned} x(t) &= e^{-\lambda t} [x_0 \cos(\omega t) - y_0 \sin(\omega t)] + o(e^{-\lambda t}) \\ y(t) &= e^{-\lambda t} [y_0 \cos(\omega t) + x_0 \sin(\omega t)] + o(e^{-\lambda t}) \\ z(t) &= e^{\gamma t} z_0. \end{aligned} \quad (5)$$

When  $\mu = 0$ , the orbit  $\Gamma$  intersects the semi-axis  $x = 0, y > 0$  in a countable set of points. We choose one of these points  $M^+(0, y^+, 0)$  and consider a two-dimensional cross-section  $\Pi^+ \{(x, y, z) | x = 0, |y - y^+| \leq \epsilon_0, 0 \leq z \leq \epsilon_0\}$ . We choose another point  $M^-(0, 0, z^-)$  on  $W_{loc}^u$ , with  $z^- > 0$ , and consider another two-dimensional cross-section  $\Pi^- \{(x, y, z) | |x| \leq \epsilon_1, |y| \leq \epsilon_1, z = z^-\}$  (figure 7).

If  $\epsilon_0$  and  $\epsilon_1$  are small enough, then the orbits of the system generate a map  $T_0 : \Pi^+ \rightarrow \Pi^-$ . According to (5), this map can be written as

$$T_0 : \Pi^+ \rightarrow \Pi^- \begin{cases} x_1 = -e^{-\lambda t_0} y_0 \sin(\omega t_0) + o(e^{-\lambda t_0}) \\ y_1 = e^{-\lambda t_0} y_0 \cos(\omega t_0) + o(e^{-\lambda t_0}) \end{cases} \quad (6)$$

where  $t_0$  is the time of flight from the point  $(0, y_0, z_0) \in \Pi^+$  to the point  $(x_1, y_1, z^-) \in \Pi^-$ . This time can be found from the last equation in (5):

$$\begin{aligned} z^- &= e^{\gamma t_0} z_0 \\ t_0 &= -\frac{1}{\gamma} \ln \frac{z_0}{z^-}. \end{aligned}$$

After the rescaling  $(x \rightarrow xy^+, y \rightarrow yy^+, z \rightarrow zz^-)$ , we obtain

$$T_0 : \Pi^+ \rightarrow \Pi^- \begin{cases} x_1 = y_0 z_0^\rho \sin\left(\frac{\omega}{\gamma} \ln z_0\right) + o(z_0^\rho) \\ y_1 = y_0 z_0^\rho \cos\left(\frac{\omega}{\gamma} \ln z_0\right) + o(z_0^\rho). \end{cases} \quad (7)$$

The orbits passing inside the handle  $U_1$  generate another map  $T_1 : \Pi^- \rightarrow \Pi^+$ . Since the time of flight is bounded for the map  $T_1$ , this map is a diffeomorphism and can be written (in the rescaled coordinates) as

$$T_1 : \Pi^- \rightarrow \Pi^+ \begin{cases} y_0 - 1 = ax_1 + by_1 + \dots \\ z_0 = \mu + cx_1 + dy_1 + \dots \end{cases} \quad (8)$$

where

$$\det \begin{pmatrix} a & b \\ c & d \end{pmatrix} \neq 0.$$

The Poincaré map  $T \equiv T_1 T_0 : \Pi^+ \rightarrow \Pi^+$  can now be defined. Combining equations (7) and (8), we obtain

$$T : \Pi^+ \rightarrow \Pi^+ \begin{cases} \bar{y}_0 = 1 + Ay_0 z_0^\rho \cos(\Omega \ln z_0 + \psi) + o(z_0^\rho) \\ \bar{z}_0 = \mu - By_0 z_0^\rho \sin(\Omega \ln z_0 + \phi) + o(z_0^\rho) \end{cases} \quad (9)$$

where  $\Omega = \omega/\gamma$ ,  $A = \sqrt{a^2 + b^2}$ ,  $B = \sqrt{c^2 + d^2}$ ,  $\cos \psi = b/A$ ,  $\sin \psi = -a/A$ ,  $\cos \phi = -c/B$ ,  $\sin \phi = -d/B$ . After the rescaling ( $z \rightarrow ze^{-\phi/\Omega}$ ,  $A \rightarrow Ae^{-\rho\phi/\Omega}$ ,  $B \rightarrow Be^{(1-\rho)\phi/\Omega}$ ,  $\mu \rightarrow \mu e^{\phi/\Omega}$ ) and omitting the lower indices, we finally obtain the following expression for the Poincaré map:

$$T : \Pi^+ \rightarrow \Pi^+ \begin{cases} \bar{y} = 1 + Ayz^\rho \cos(\Omega \ln z + \theta) + o(z^\rho) \\ \bar{z} = \mu - Byz^\rho \sin(\Omega \ln z) + o(z^\rho) \end{cases} \quad (10)$$

where  $A \neq 0$ ,  $B \neq 0$ ,  $\theta = \psi - \phi$ ,  $\cos \theta \neq 0$ .

### 3. The double-circuit loops

According to equation (8), the separatrix  $\Gamma$  intersects  $\Pi^+$  at the point:  $M^+(\mu) = (0, 1, \mu)$ . The next point of intersection (i.e. the point  $TM^+(\mu)$ ) has the coordinates

$$\begin{cases} \bar{y} = 1 + A\mu^\rho \cos(\Omega \ln \mu + \theta) + o(\mu^\rho) \\ \bar{z} = \mu - B\mu^\rho \sin(\Omega \ln \mu) + o(\mu^\rho). \end{cases} \quad (11)$$

The condition of existence of a double-circuit homoclinic loop is  $TM^+ \in W_{\text{loc}}^s$ ; i.e.  $\bar{z} = 0$ . It follows from equation (11) that the bifurcation set corresponding to the existence of double-circuit loops is defined by the equation

$$\mu = B\mu^\rho \sin(\Omega \ln \mu) + o(\mu^\rho). \quad (12)$$

To isolate its solutions, we assume

$$\Omega \ln \mu = -2\pi j + \xi$$

or

$$\mu = e^{-2\pi j/\Omega} e^{\xi/\Omega} \quad (13)$$

where  $j$  is an integer (large enough since  $\mu$  should be small), and  $\xi$  belongs to the interval  $[-\frac{\pi}{2}, \frac{3\pi}{2}]$ . Equation (12) is rewritten as

$$\sin \xi = \frac{1}{B} e^{-\frac{2\pi j}{\Omega}(1-\rho)} e^{\xi \frac{1-\rho}{\Omega}} + o[e^{-\frac{2\pi j}{\Omega}(1-\rho)}]. \quad (14)$$

Since  $\rho < 1$ , the quantity  $e^{-\frac{2\pi j}{\Omega}(1-\rho)}$  is small when  $j$  is large. Hence, equation (14) has exactly two solutions on the interval  $-\frac{\pi}{2} \leq \xi < \frac{3\pi}{2}$ :

$$\begin{aligned} \xi_0 &= \pi - \frac{1}{B} e^{-\frac{2\pi j}{\Omega}(1-\rho)} e^{\pi \frac{1-\rho}{\Omega}} + \dots \\ \xi_1 &= \frac{1}{B} e^{-\frac{2\pi j}{\Omega}(1-\rho)} + \dots \end{aligned}$$



Substituting these expressions into equation (13), we find that an infinite series of bifurcation curves  $\{L_j^0, L_j^1\}$  corresponds to the existence of double-circuit loops:

$$\begin{aligned} L_j^0 : \mu &= e^{-\frac{2\pi j}{\Omega}} e^{\frac{\pi}{\Omega}} \left[ 1 - \frac{1}{B\Omega} e^{-\frac{2\pi j}{\Omega}(1-\rho)} e^{\pi \frac{1-\rho}{\Omega}} + \dots \right] \\ L_j^1 : \mu &= e^{-\frac{2\pi j}{\Omega}} \left[ 1 + \frac{1}{B\Omega} e^{-\frac{2\pi j}{\Omega}(1-\rho)} + \dots \right]. \end{aligned} \quad (15)$$

Note that, in the region bounded by  $L_j^0$  and  $L_j^1$  (the shaded regions in figure 5), the system  $X_{\mu,\rho}$  does not have homoclinic loops since here  $\bar{z} < 0$  (see equation (11)) which means that the separatrix  $\Gamma$  passes below  $W_{\text{loc}}^s$  and leaves  $U$  after the first passage along  $U_1$ . On the other hand, there is a complicated set of bifurcation curves of triple- and higher multi-circuit loops between  $L_{j+1}^0$  and  $L_j^1$ , as shown below.

#### 4. The triple-circuit loops

A triple-circuit loop intersects  $\Pi^+$  at the three points:  $M^+ = (0, 1, \mu)$ ,  $TM^+ = (0, y_1, z)$  and  $T^2M^+ = (0, y_2, 0) \in W_{\text{loc}}^s$ . From equation (10), we have

$$\begin{aligned} y_1 &= 1 + A\mu^\rho \cos(\Omega \ln \mu + \theta) + o(\mu^\rho) \\ z &= \mu - B\mu^\rho \sin(\Omega \ln \mu) + o(\mu^\rho) \\ 0 &= \mu - Bz^\rho \sin(\Omega \ln z) + o(z^\rho). \end{aligned}$$

Expressing  $y_1$  by the first equation, we arrive at the following equations determining the bifurcation curves of triple-circuit loops

$$\begin{cases} z = \mu - B\mu^\rho \sin(\Omega \ln \mu) + o(\mu^\rho) \\ \mu = Bz^\rho \sin(\Omega \ln z) + o(z^\rho). \end{cases} \quad (16)$$

We study these equations by means of the following assumption

$$\begin{aligned} \Omega \ln \mu &= -2\pi j + \xi & \text{where } -\frac{3\pi}{2} \leq \xi < \frac{\pi}{2} \\ \Omega \ln z &= -2\pi k + \eta & \text{where } 0 \leq \eta < 2\pi \end{aligned} \quad (17)$$

which is similar to the assumption we used while studying double-circuit loops in the previous section. We choose the interval  $[-\frac{3\pi}{2}, \frac{\pi}{2}]$  to be the range of  $\xi$  since we are interested in the values of  $\mu$  lying between  $L_{j+1}^0$  and  $L_j^1$  (see equation (15)). Equations (16) take the form

$$\begin{aligned} \sin \xi &= \frac{1}{B} (e^{-2\pi j/\Omega} e^{\xi/\Omega} - e^{-2\pi k/\Omega} e^{\eta/\Omega}) e^{2\pi j\rho/\Omega} e^{-\rho\xi/\Omega} + \dots \\ \sin \eta &= \frac{1}{B} e^{\frac{2\pi}{\Omega}(\rho k - j)} e^{(\xi - \rho\eta)/\Omega} + \dots \end{aligned} \quad (18)$$

where the dots stand for higher-order terms.

There are three different cases: (1)  $j = k$ , (2)  $j > k$ , and (3)  $j < k$ ; we consider them separately.

**Case 1.** When  $j = k$ , the system (18) can be written in the form

$$\begin{aligned} \sin \xi &= \frac{1}{B} e^{-\frac{2\pi j}{\Omega}(1-\rho)} (e^{\frac{\xi}{\Omega}} - e^{\frac{\eta}{\Omega}}) e^{-\frac{\rho\xi}{\Omega}} + \dots \\ \sin \eta &= \frac{1}{B} e^{-\frac{2\pi j}{\Omega}(1-\rho)} e^{\frac{\xi - \rho\eta}{\Omega}} + \dots \end{aligned} \quad (19)$$

Since  $0 \leq \eta < 2\pi$ , the second equation in (19) has exactly two solutions:

$$\begin{aligned}\eta_0 &= \frac{1}{B} e^{-2\pi j(1-\rho)/\Omega} e^{\xi/\Omega} + \dots \\ \eta_1 &= \pi - \frac{1}{B} e^{-2\pi j(1-\rho)/\Omega} e^{\frac{\xi-\rho\pi}{\Omega}} + \dots\end{aligned}$$

for any  $\xi \in [-\frac{3\pi}{2}, \frac{\pi}{2}[$  and integer  $j$  large enough.

Let us substitute  $\eta = \eta_0$  in the first equation of (19). We have

$$\sin \xi = \frac{1}{B} e^{-\frac{2\pi j}{\Omega}(1-\rho)} \left[ e^{\frac{\xi}{\Omega}} - 1 - \frac{1}{B\Omega} e^{-\frac{2\pi j}{\Omega}(1-\rho)} e^{\frac{\xi}{\Omega}} - \dots \right] e^{-\frac{\rho\xi}{\Omega}}. \quad (20)$$

This equation has two solutions in the interval  $[-\frac{3\pi}{2}, \frac{\pi}{2}[$ :

$$\begin{aligned}\xi_{00} &= -\frac{1}{B^2\Omega} e^{-4\pi j(1-\rho)/\Omega} + \dots \\ \xi_{01} &= -\pi + \frac{1}{B} e^{-2\pi j(1-\rho)/\Omega} (1 - e^{-\pi/\Omega}) e^{\rho\pi/\Omega} + \dots.\end{aligned}$$

Assuming  $\eta = \eta_1$  we arrive at an equation similar to (20)

$$\sin \xi = \frac{1}{B} e^{-\frac{2\pi j}{\Omega}(1-\rho)} \left\{ e^{\frac{\xi}{\Omega}} - e^{\frac{\pi}{\Omega}} \left[ 1 - \frac{1}{B\Omega} e^{-\frac{2\pi j}{\Omega}(1-\rho)} e^{\frac{\xi-\rho\pi}{\Omega}} - \dots \right] \right\} e^{-\frac{\rho\xi}{\Omega}}$$

which has also two solutions:

$$\begin{aligned}\xi_{10} &= -\frac{1}{B} e^{-2\pi j(1-\rho)/\Omega} (e^{\pi/\Omega} - 1) + \dots \\ \xi_{11} &= -\pi + \frac{1}{B} e^{-2\pi j(1-\rho)/\Omega} (e^{2\pi/\Omega} - 1) e^{-(1-\rho)\pi/\Omega} + \dots.\end{aligned}$$

When  $j = k$ , the corresponding bifurcation set therefore consists of four branches for each integer  $j$  large enough. These four branches are given by the equation

$$\mu_{\alpha_1, \alpha_2} = e^{-\frac{2\pi j}{\Omega}} e^{\frac{\xi_{\alpha_1, \alpha_2}}{\Omega}} \quad \text{with } \alpha_1, \alpha_2 = 0, 1.$$

**Case 2.** When  $j > k$ , the system (18) can be rewritten as

$$\begin{aligned}\sin \xi &= -\frac{1}{B} e^{-\frac{2\pi}{\Omega}(k-\rho j)} e^{\frac{\eta-\rho\xi}{\Omega}} [1 - e^{-\frac{2\pi}{\Omega}(j-k)} e^{\frac{\xi-\eta}{\Omega}}] + \dots \\ \sin \eta &= \frac{1}{B} e^{-\frac{2\pi}{\Omega}(j-\rho k)} e^{\frac{\xi-\rho\eta}{\Omega}} + \dots.\end{aligned} \quad (21)$$

Note that the value  $(j - \rho k)$  is very large since  $0 < \rho < 1$  and  $k < j$ , so that the coefficient  $e^{-\frac{2\pi}{\Omega}(j-\rho k)}$  is very small. Therefore, the second equation in (21) can be resolved with respect to  $\eta$ :

$$\begin{aligned}\eta_0 &= \frac{1}{B} e^{-\frac{2\pi}{\Omega}(j-\rho k)} e^{\frac{\xi}{\Omega}} + \dots \\ \eta_1 &= \pi - \frac{1}{B} e^{-\frac{2\pi}{\Omega}(j-\rho k)} e^{\frac{\xi-\rho\pi}{\Omega}} + \dots.\end{aligned} \quad (22)$$

Let us substitute  $\eta = \eta_0$  in the first equation in (21). We obtain

$$e^{\frac{\rho\xi}{\Omega}} \sin \xi = -C(\rho, \xi) \quad (23)$$

where

$$C(\rho, \xi) = \frac{1}{B} e^{-\frac{2\pi}{\Omega}(k-\rho j)} [1 - e^{-\frac{2\pi}{\Omega}(j-k)} e^{\frac{\xi}{\Omega}}] + \dots > 0. \quad (24)$$

When  $C$  is close to zero ( $(k-\rho j)$  is large), equation (23) has two solutions corresponding to the two branches of the bifurcation curve  $L_{jk}^0$  while the equation has no solutions when  $C$  is large. The solutions merge at some intermediate value of  $C$  which corresponds to the case where  $k$  is close to  $\rho j$ . Since we suppose  $j$  and  $k$  to be very large, it means that  $(j-k)$  is very large in this case. Thus, the graph of the function  $C(\xi)$  is close to the straight line

$$C(\xi) = \frac{1}{B} e^{-\frac{2\pi}{\Omega}(k-\rho j)} \tag{25}$$

at the moment of merging. Therefore, the solutions merge near the minimum point  $\xi^* = -\arctan \frac{\Omega}{\rho}$  of the right-hand side of (23). The corresponding value of  $\rho$  can be found with substituting  $\xi = \xi^*$  in (23) and, after simple calculations, we obtain

$$\rho = \rho_{jk0}^* = \frac{k}{j} + \frac{\tau}{j} + \dots$$

where

$$\tau = \frac{1}{2\pi} \left( \Omega \ln \frac{B\Omega}{\sqrt{\Omega^2 + \rho^2}} - \rho \arctan \frac{\Omega}{\rho} \right). \tag{26}$$

This value of  $\rho$  corresponds to the merging of the two branches  $\mu_{1,2} = e^{-\frac{2\pi j}{\Omega}} e^{\frac{\xi_{1,2}}{\Omega}}$  of the curve  $L_{jk}^0$ , where the curve has a vertical tangent.

Analogously, one can find that the curve  $L_{jk}^1$  defined by the first equation in (21) at  $\eta = \eta_1$ , has a vertical tangent at

$$\rho = \rho_{jk1}^* = \frac{k}{j} + \frac{\tau - \frac{1}{2}}{j} + \dots$$

**Case 3.** To complete the bifurcation diagram for triple-circuit loops we have still to consider the case  $j < k$ . Here, the system (18) is rewritten as

$$\begin{aligned} \sin \xi &= \frac{1}{B} e^{-\frac{2\pi j}{\Omega}(1-\rho)} e^{\frac{\xi(1-\rho)}{\Omega}} [1 - e^{-\frac{2\pi}{\Omega}(k-j)} e^{\frac{\eta-\xi}{\Omega}}] + \dots \\ \sin \eta &= \frac{1}{B} e^{-\frac{2\pi}{\Omega}(j-\rho k)} e^{\frac{\xi-\rho\eta}{\Omega}} + \dots \end{aligned} \tag{27}$$

The first equation always has two solutions in the interval  $[-\frac{3\pi}{2}, \frac{\pi}{2}]$ :

$$\begin{aligned} \xi_0 &= \frac{1}{B} e^{-\frac{2\pi j}{\Omega}(1-\rho)} [1 - e^{-\frac{2\pi}{\Omega}(k-j)} e^{\frac{\eta}{\Omega}}] + \dots \\ \xi_1 &= -\pi - \frac{1}{B} e^{-\frac{2\pi j}{\Omega}(1-\rho)} e^{-\frac{\pi(1-\rho)}{\Omega}} [1 - e^{-\frac{2\pi}{\Omega}(k-j)} e^{\frac{\eta+\pi}{\Omega}}] + \dots \end{aligned} \tag{28}$$

These solutions define the bifurcation curves  $L_{jk}^0$  and  $L_{jk}^1$ , respectively. It is easy to calculate that  $L_{jk}^0$  has a vertical tangency at

$$\rho = \rho_{jk0}^* = \frac{j}{k - \frac{1}{2}} + \frac{\tau}{k} + \dots$$

and  $L_{jk}^1$  at

$$\rho = \rho_{jk1}^* = \frac{j}{k - \frac{1}{2}} + \frac{\tau + \frac{1}{2}}{k} + \dots$$

We have obtained a complete description of the bifurcation set corresponding to triple-circuit loops. Theorem 1 presented in the introduction is a direct consequence of our

considerations: for any one-parameter family  $\rho = \varphi(\mu)$  and for arbitrarily small  $\delta > 0$  there exist large enough integers  $j$  and  $k$  such that the curve  $L_{jk}^0$  intersects the curve  $\rho = \varphi(\mu)$  and does not intersect the curve  $\rho = \varphi(\mu) + \delta$  (given that  $\rho_{jk0}^* \in ]\varphi(0), \varphi(0) + \delta[$ ) which implies that  $L_{jk}^0$  have a tangency with the curve  $\rho = \varphi(\mu) + \delta^*$  for some  $\delta^* \in ]0, \delta[$ .

**5. The multi-circuit loops**

We have seen in the previous section that any one-parameter family transverse to the line of single-circuit loops can be made tangential to some line of triple-circuit loops by an arbitrarily small smooth perturbation. Before going further, we consider what happens under small perturbations of a one-parameter family which is non-transverse to the line of single-circuit loops.

**Lemma.** *Let a smooth one-parameter family  $\mu = \psi(\rho)$  have a tangency of order  $(n - 1)$  with the line  $\mu = 0$  of single-circuit loops at some point  $\rho = \rho_0$ . Then, by an arbitrarily small smooth perturbation of the function  $\psi$ , the family can be made tangential to some line of triple-circuit loops and the tangency is of order  $n$ .*

**Proof.** Near the point  $(\rho = \rho_0, \mu = 0)$ , the family under consideration can be written in the form

$$\mu = (\rho - \rho_0)^n + o(\rho - \rho_0)^n.$$

We consider the following perturbed family

$$\mu = \sum_{j=0}^{n-2} \epsilon_j (\rho - \rho_0 - \delta)^j + (\rho - \rho_0 - \delta)^n + o(\rho - \rho_0)^n \tag{29}$$

where  $\delta$  and  $\epsilon_j, j = 0, \dots, n - 2$ , are small values which should be determined.

Let  $\{k_m, j_m\}$  be a sequence of pairs of integers such that  $j_m \rightarrow \infty, k_m \rightarrow \infty, \frac{k_m}{j_m} \rightarrow \rho_0$  as  $m \rightarrow \infty$ . Then, as it follows from the previous section, there exists in the parameter plane a set of points  $\{\rho_m, \mu_m\}, \rho_m \rightarrow \rho_0, \mu_m \rightarrow 0$ , such that a line of existence of a triple-circuit loop  $\Gamma_{j_m k_m}$  have a vertical tangency at the point  $\{\rho_m, \mu_m\}$ . We infer from equation (23) that, near the point of tangency, the equation of this line is written in the form

$$\rho = \frac{k_m}{j_m} + \frac{\tau - D_0(\xi - \xi^*)^2 + \dots}{j_m} \tag{30}$$

where the variable  $\xi$  is connected with  $\mu$  by equation (17),  $\xi^* = -\arctan \frac{\Omega}{\rho_0}$  is the minimum point of the function  $e^{\frac{\rho_0 \xi}{\Omega}} \sin \xi$ ,  $D_0$  is some positive constant, and the dots denote terms smaller than those explicitly written down.

We intend to deal with a small neighbourhood of the point  $(\rho = \rho_0, \mu = 0)$  which means that  $j_m$  should be large enough, and also with a small neighbourhood of the top of parabola  $L_{j_m k_m}^0$  which means that  $\xi$  is close to  $\xi^*$ . In this respect, let us make a change of variables

$$\xi = \xi^* + \alpha u \quad \rho = \rho_0 + \delta + \beta v$$

where  $\alpha$  and  $\beta$  are small scaling parameters. Equations (30) and (29) now take the form

$$\beta v = \left( \frac{k_m}{j_m} - \rho_0 - \delta + \frac{\tau}{j_m} \right) - D_0 \frac{(\alpha u)^2}{j_m} + o\left(\frac{\alpha^2}{j_m}\right) \tag{31}$$

$$\frac{\alpha}{\Omega} e^{\frac{-2\pi j_m + \xi^*}{\Omega}} u [1 + o(\alpha)] = \left( \epsilon_0 - e^{\frac{-2\pi j_m + \xi^*}{\Omega}} \right) + \sum_{j=1}^{n-2} \epsilon_j (\beta v)^j + (\beta v)^n + o(\beta^n). \tag{32}$$

Assume

$$\beta = D_0 \frac{\alpha^2}{j_m} \quad \frac{\alpha}{\Omega} e^{\frac{-2\pi j_m + \xi^*}{\Omega}} = \beta^n$$

or, equivalently,

$$\beta^{2n-1} = \frac{j_m}{\Omega^2 D_0} e^{2\frac{-2\pi j_m + \xi^*}{\Omega}} \quad \alpha^{2n-1} = \frac{(j_m)^n}{\Omega D_0^n} e^{\frac{-2\pi j_m + \xi^*}{\Omega}}$$

with  $\alpha \rightarrow 0$  and  $\beta \rightarrow 0$  as  $m \rightarrow \infty$ . As a consequence, equations (31) and (32) take the form

$$v = \Delta - u^2 + \dots \quad (33)$$

$$u = \sum_{j=0}^{n-2} E_j v^j + v^n + \dots \quad (34)$$

where  $\Delta$  and  $E_j$  are rescaled parameters which are no longer small and can take arbitrary values; the dots denote terms which tends to zero as  $\alpha$  and  $\beta$  tend to zero, i.e. these terms can be made as small as necessary for  $j_m$  large enough. Our aim is now to find the values of  $\Delta$  and  $E_j$  for which the curves defined in the plane  $(u, v)$  by equations (33) and (34) have a tangency of order  $n$  for some  $(u = u^*, v = v^*)$ .

The condition of the tangency is

$$\begin{aligned} v^* &= \Delta - P^2(v^*) + \dots \\ 1 &= -2P(v^*)P'(v^*) + \dots \\ 0 &= -P(v^*)P''(v^*) - [P'(v^*)]^2 + \dots \\ &\dots \\ 0 &= -\frac{d^n P^2}{dv^n}(v^*) + \dots \end{aligned} \quad (35)$$

where  $P(v) = \sum_{j=0}^{n-2} E_j v^j + v^n$ . It is easy to find from this equation that

$$\begin{aligned} P'(v^*) &= -1/[2P(v^*)] + \dots \\ P''(v^*) &= -1/[4[P(v^*)]^3] + \dots \\ &\dots \\ P^{(j)}(v^*) &= -\sigma_j/[P(v^*)]^{2j-1} + \dots \\ &\dots \\ P^{(n)}(v^*) &= -\sigma_n/[P(v^*)]^{2n-1} + \dots \end{aligned} \quad (36)$$

where  $\sigma_j$  are positive constants. We use the identity

$$P(v) = P(v^*) + P'(v^*)(v - v^*) + \dots + \frac{1}{n!} P^{(n)}(v^*)(v - v^*)^n \quad (37)$$

valid for any polynomial of degree  $n$ . Since the coefficient of  $v^n$  is equal to 1 and the coefficient of  $v^{n-1}$  to 0 for the present polynomial  $P(v)$ , it follows from equation (37) that

$$P^{(n)}(v^*) = n! \quad (38)$$

$$P^{(n-1)}(v^*) = v^* P^{(n)}(v^*). \quad (39)$$

Now, we deduce from the last equation of (36) that

$$P(v^*) = -\left(\frac{\sigma_n}{n!}\right)^{1/(2n-1)} + \dots$$

and we can similarly calculate the values of the derivatives  $P^{(j)}(v^*)$  from equations (36). Thereafter, the required values of the parameters  $E_j$  are obtained from identity (37). The last step is to find the value  $v^*$  from equation (39) and, then, to calculate  $\Delta$  from the first equation of (35).

Accordingly, we have the parameter values for which conditions (35) are satisfied. Returning to the non-rescaled variables, we obtain the values of  $\epsilon_j$  and  $\delta$  for which the curve (29) has a tangency of the  $n$ th order with the curve  $L_{j_m k_m}^0$ , which proves the lemma.

At this stage, we are prepared to prove theorem 2 of this paper. Consider an arbitrary one-parameter family transverse to the line of single-circuit loops. By a small perturbation, we can obtain a tangency with some line  $\mathcal{L}$  of some triple-circuit loop  $\Gamma'$ . We assume that the point of tangency,  $M$ , does not coincide with the point where  $\mathcal{L}$  has a vertical tangency: if it did happen we could avoid this coincidence by slightly perturbing the one-parameter family in order to move the point  $M$  along  $\mathcal{L}$ . Therefore, we can assume that, near  $M$ , the value  $\rho$  changes monotonically along  $\mathcal{L}$ .

Consider a small neighbourhood of  $M$  in the parameter plane and take the loop  $\Gamma'$  as the initial single-circuit loop. Then, due to the lemma, there exists a small perturbation under which our one-parameter family have a cubic tangency with some curve of homoclinic loops which are triple-circuit with respect to  $\Gamma'$  or nine-circuit with respect to the loop  $\Gamma$ . Applying the lemma again, we can obtain (by small perturbation of the family) a tangency of third order with a line of 27-circuit loops. Continuing this inductive reasoning, we obtain a tangency of order  $n$  with a line of  $3^n$ -circuit loops, which ends the proof of theorem 2.

## 6. Concluding remarks

In this paper, we showed the high structural instability of one-parameter families of vector fields near homoclinic loops to a saddle-focus. Some comments are now in order about the consequences of these results.

It was proved elsewhere [23] that the values of  $\rho$  for which the system has a structurally unstable Poincaré homoclinic curve at  $\mu = 0$  are dense. This implies, in agreement with [14], that the bifurcations of the periodic orbits belonging to the neighbourhood  $U$  of the homoclinic loop cannot be completely studied in any finite-parameter family. This result showed a fundamental incompleteness in the topological description of periodic orbits in the vicinity of structurally unstable homoclinic orbits. A complementary aspect of this result is provided by theorem 2 of the present paper, which suggests that the complete description of the structure of the bifurcation set corresponding to multi-circuit homoclinic loops to a saddle-focus can never be achieved with a finite number of parameters.

Theorems 1 and 2 can also be applied to the theory of nonlinear partial differential equations modelling travelling waves in spatially extended systems. Let us imagine that  $X_{\mu,\rho}$  is a family of ordinary differential equations describing the plane travelling waves of some distributed system in a frame moving with the wavefront;  $\mu$  is the wave velocity while  $\rho$  is an internal parameter of the system. Let the saddle-focus  $O$  be at the origin. It is known that homoclinic loops correspond to self-localized waves in such systems [17–19]. Suppose that the system has such a wave and that conditions A–C of the introduction are fulfilled for some parameter value  $\mu = \mu_0$ . It follows from theorem 1 that bifurcations generating ‘three-pulsed’ self-localized travelling waves occur for arbitrary small variations of  $\rho$  in this system. In turn, theorem 2 implies that the complete description of bifurcations of plane self-localized waves is impossible in systems of such kind.

## Acknowledgments

The authors would like to thank Professor L P Shil'nikov for many useful discussions. PG thanks the National Fund for Scientific Research (FNRS Belgium) for financial support. This work is financially supported by the European Commission contract No ECRU002 and by the International Science Foundation (ISF) grant No R98000.

## References

- [1] Afrajmovich V S, Arnold V I, Il'yashenko Yu S and Shil'nikov L P 1994 *Dynamical Systems V: Bifurcation Theory and Catastrophe Theory* (Berlin: Springer)
- [2] Hao Bai-Lin (ed) 1984, 1990 *Chaos I & II* Reprint collections (Singapore: World Scientific)
- [3] Shil'nikov L P 1965 A case of the existence of a countable number of periodic motions *Sov. Math. Dokl.* **6** 163
- [4] Shil'nikov L P 1972 On the question of the structure of an extended neighborhood of a rough saddle-node equilibrium *Math. USSR Sb.* **10** 91–102
- [5] Gavrilov N K and Shilnikov L P 1973 Three-dimensional dynamical systems that are close to systems with a structurally unstable homoclinic curve I *Math. USSR Sb.* **17** 467–85
- [6] Gavrilov N K and Shilnikov L P 1974 Three-dimensional dynamical systems that are close to systems with a structurally unstable homoclinic curve II *Math. USSR Sb.* **19** 139–56
- [7] Gumowski I and Mira C 1980 *Dynamique Chaotique* (Toulouse: Cepadues Editions)
- [8] Afrajmovich V S, Bykov V S and Shil'nikov L P 1983 On structurally unstable attracting limit sets of Lorenz attractor type *Trans. Moscow Math. Soc.* **2** 153–216
- [9] Arnéodo A, Couillet P and Tresser C 1982 Oscillators with Chaotic Behaviour: An Illustration of a Theorem by Shil'nikov *J. Stat. Phys.* **27** 171–82
- [10] Gaspard P and Nicolis G 1983 What can we learn from homoclinic orbits in chaotic dynamics? *J. Stat. Phys.* **31** 499–518
- [11] Sparrow C T 1982 *The Lorenz Equations: Bifurcations, Chaos, and Strange Attractors* (Berlin: Springer)
- [12] Newhouse S 1974 Diffeomorphisms with infinitely many sinks *Topology* **13** 9–18
- [13] Robinson C 1983 Bifurcation to infinitely many sinks *Commun. Math. Phys.* **90** 433–59
- [14] Gonchenko S V, Shil'nikov L P and Turaev D V 1993 On models with non-rough Poincaré homoclinic curves *Physica D* **62** 1–14
- [15] Gonchenko S V, Turaev D V and Shil'nikov L P 1993 Dynamical phenomena in multi-dimensional systems with a non-rough Poincaré homoclinic curves *Dokl. RAN* **330** 144–7 (in Russian)
- [16] Gaspard P 1983 Generation of a countable set of homoclinic flows through bifurcation *Phys. Lett.* **97A** 1–4
- [17] Evans J W, Fenichel N and Feroe J A 1982 Double impulse solutions in nerve axon equations *SIAM J. Appl. Math.* **42** 219–34
- [18] Feroe J A 1982 Existence and stability of multiple impulse solutions of a nerve equation *SIAM J. Appl. Math.* **42** 235–46
- Feroe J A 1993 Homoclinic orbits in a parametrized saddle-focus system *Physica D* **62** 254–62
- [19] Hastings S P 1982 Single and multiple pulse waves for the FitzHugh–Nagumo equations *SIAM J. Appl. Math.* **42** 247–60
- [20] Belyakov L 1974 A case of the generation of a periodic orbit motion with homoclinic curves *Mat. Zam.* **15** 336–41
- [21] Belyakov L 1984 Bifurcation of systems with homoclinic curve of a saddle-focus with saddle quantity zero *Mat. Zam.* **36** 838–43
- [22] Belyakov L A and Shil'nikov L P 1990 Homoclinic curves and complex solitary waves *Selecta Math. Sov.* **9** 219–28
- [23] Ovsyannikov I M and Shil'nikov L P 1986 On systems with a saddle-focus homoclinic curve *Mat. Sb.* **130** 552–70 (Engl. transl. 1987 *Math. USSR Sb.* **58**)
- [24] Ovsyannikov I M and Shil'nikov L P 1992 Systems with a homoclinic curve of multidimensional saddle-focus type, and spiral chaos *Math. USSR Sb.* **73** 415–43